

Published in final edited form as:

*Eur J Neurosci.* 2009 January ; 29(1): 42–54. doi:10.1111/j.1460-9568.2008.06563.x.

## Calcyon is Necessary for Activity Dependent AMPA Receptor Internalization and LTD in CA1 Neurons of Hippocampus

Heather Trantham Davidson<sup>1,2</sup>, Jiping Xiao<sup>1,3</sup>, Rujuan Dai<sup>1,4</sup>, and Clare Bergson<sup>1</sup>

<sup>1</sup> Department of Pharmacology and Toxicology, Medical College of Georgia

### Abstract

Calcyon is a single transmembrane endocytic protein that regulates clathrin assembly and clathrin mediated endocytosis in brain. Ultrastructural studies indicate that calcyon localizes to spines, but whether it regulates glutamate neurotransmission is not known. Here, we show that deletion of the calcyon gene in mice inhibits agonist stimulated endocytosis of AMPA receptors, without altering basal surface levels of the GluR1 or GluR2 subunits. Whole cell patch clamp studies of hippocampal neurons in culture and CA1 synapses in slices revealed that knockout of calcyon abolishes long term synaptic depression (LTD) whereas mini-analysis in slices indicated basal transmission in hippocampus is unaffected by the deletion. Further, transfection of GFP-tagged calcyon rescued the ability of knockout cultures to undergo LTD. In contrast, intracellular dialysis of a fusion protein containing the clathrin light chain binding domain of calcyon blocked the induction of LTD in wild type hippocampal slices. Taken together, the present studies involving biochemical, immunological and electrophysiological analyses raise the possibility that calcyon plays a specialized role in regulating activity-dependent removal of synaptic AMPA receptors.

### Keywords

synaptic plasticity; glutamate transmission; clathrin mediated endocytosis; ADHD; schizophrenia

### Introduction

One of the most interesting characteristics of synapses lies in their ability to differentially respond following variations in afferent input, a property known as synaptic plasticity. Synaptic plasticity is a proposed neural correlate of learning and memory, and has been extensively characterized in the hippocampus (Ito 1989; Lynch and Baudry 1984; Teyler and Discenna 1984; Kesner and Rolls 2001). Long-term potentiation (LTP) and long-term depression (LTD), the best characterized forms of plasticity, are evoked by distinct patterns of activity, and result in synaptic strengthening and weakening, respectively.

Numerous studies indicate that a common postsynaptic mechanism of LTP and LTD involves a net change in the number of synaptic AMPA ( $\alpha$ -amino-3-hydroxy-5-methyl-4-isoxazolepropionic acid)-type glutamate receptors (AMPA receptors). Functional AMPARs are heteromeric tetramers assembled from a combination of four different subunits (GluR1-GluR4). Native receptors in hippocampus are comprised mainly of GluR1/R2 or GluR2/R3

Address correspondence to: Clare M. Bergson, Department of Pharmacology and Toxicology, Medical College of Georgia, 1459 Laney Walker Blvd, Augusta, GA 30912-2300. Tel: 706-721-1926; Fax: 706-721-2347; cbergson@mail.mcg.edu.

<sup>2</sup>Present address: Department of Neuroscience, Medical University of South Carolina, Charleston, South Carolina

<sup>3</sup>Present address: Center for Neurodegenerative Disease Research, University of Pennsylvania, Philadelphia, PA

<sup>4</sup>Present address: Department of Biomedical Sciences and Pathobiology, Virginia Polytechnic Institute and State University, Blacksburg, Virginia 24061

subunits (Wenthold *et al.*, 1996). In addition to activity-regulated insertion and removal from synapses, AMPARs constitutively cycle into the synapse (Shi *et al.*, 2001;Lin *et al.*, 2000;Noel *et al.*, 1999). Constitutive exocytosis and receptor insertion into synapses appears to be balanced by endocytosis (Luscher *et al.*, 1999). Presumably, stimuli that evoke LTP or LTD effect net changes in synaptic strength by altering the relative rates of GluR synaptic insertion and removal, endocytic sorting decisions (Steiner *et al.*, 2002;Steiner *et al.*, 2005), biosynthesis, degradation, and/or the numbers of 'slots' available for retaining AMPARs at synapses (Malinow 2003).

Recent studies into the mechanisms underlying LTP and LTD have highlighted a crucial role for a range of proteins, both ubiquitous as well as neural-specific, involved in vesicle trafficking (Noel *et al.*, 1999;Chowdhury *et al.*, 2006;Luscher *et al.*, 1999;Carroll *et al.*, 1999a;Park *et al.*, 2004;Palmer *et al.*, 2005;Brown *et al.*, 2005;Alberi *et al.*, 2005). Among the neural-specific endosomal proteins that have emerged from this area of research is NEEP21, a member of a relatively uncharacterized family of single transmembrane proteins that also includes calcyon and P19 (Steiner *et al.*, 2002;Saberan-Djoneidi *et al.*, 1995;Saberan-Djoneidi *et al.*, 1998;Xiao *et al.*, 2006;Xiao *et al.*, 2006). NEEP21 regulates the endocytic sorting and recycling of internalized GluR2-containing AMPA receptors (Saberan-Djoneidi *et al.*, 1998;Steiner *et al.*, 2002;Steiner *et al.*, 2005). In addition, knockdown of NEEP21 prevents stable LTP in hippocampus (Alberi *et al.*, 2005). The related protein calcyon stimulates clathrin assembly and clathrin mediated endocytosis in brain, presumably via a direct interaction with clathrin light chain (LC) (Xiao *et al.*, 2006). Intriguingly, clathrin mediated endocytosis is a key step both in the constitutive cycling as well as activity dependent removal of synaptic AMPA receptors (Carroll *et al.*, 1999b;Man *et al.*, 2000;Wang and Linden 2000). However, while calcyon is expressed in hippocampus and localizes near excitatory synapses (Xiao *et al.*, 2006;Zelenin *et al.*, 2002;Oakman and Meador-Woodruff 2004), it is not known whether calcyon regulates glutamate transmission or synaptic plasticity. Here, we asked whether calcyon regulates either process in studies using brain slices and neurons cultured from calcyon knockout mice. Data obtained from biochemical, immunological as well as electrophysiological analyses point to a role for calcyon in agonist-stimulated and activity dependent, but not constitutive, internalization of AMPARs. Altogether these studies suggest that in hippocampus, calcyon plays a crucial role in synaptic weakening by facilitating AMPAR internalization in response to LTD-inducing stimuli.

## Materials and Methods

### Animals

Calcyon knockout ( $Cal^{-/-}$ ) and wild type (WT or  $Cal^{+/+}$ ) littermates (Xiao *et al.*, 2006) were bred on a C57Bl/6 background, and maintained in the animal facility at Medical College of Georgia. All animal experiments were conducted with protocols approved by of the Animal Care and Use Committee in accordance with the Public Health Service Guidelines.

### Neuronal cultures

Neurons were isolated from the hippocampus of E16 mice using a protocol modified from (Redmond *et al.*, 2002) and (Lin *et al.*, 2000). Cells were plated in 24 wells at  $2 \times 10^4$ /well on coverslips coated with poly-L-lysine and laminin, or seeded at  $1.5 \times 10^6$ /60mm plate in the basal Eagle's medium containing 1 mM L-glutamine, 5% fetal bovine serum. The media was changed 1–2 hours after plating to growth media (Neurobasal media supplemented with B-27 (1:50), 0.5 mM L-glutamine and 12.5  $\mu$ M glutamate). For studies involving EGFP-calcyon plasmid DNA transfection, the hippocampal neurons were plated at density of

$2 \times 10^5$ /well on coverslips, and transfected at 14 DIV using the calcium phosphate method as described (Redmond *et al.*, 2002). Recordings were performed 1–6 days post-transfection.

### Whole cell patch clamp recordings

Electrophysiological recordings of neurons in primary cultures were conducted between 12 and 18 DIV. Coverslips were submerged in a recording chamber placed on the stage of a Zeiss Axiovert 100 microscope, and continuously perfused at a rate of 1.5 ml/min with recording ACSF (pH 7.4) containing (in mM): 120 NaCl, 5 KCl, 5 HEPES, 20 glucose, 25 sucrose, 1.8 CaCl<sub>2</sub>, 1.0 MgCl<sub>2</sub>. Neurons were viewed under brightfield or epifluorescence illumination at 20X magnification. Whole cell patch clamp recordings were obtained at room temperature (25–28°C) using thin walled glass pipettes (3–5 MΩ), filled with (in mM): 125 Potassium gluconate, 20 KCl, 1 EGTA, 2 MgCl<sub>2</sub>, 10 HEPES, 2 ATP, 0.5 GTP, and 10 phosphocreatine. To isolate miniature excitatory postsynaptic currents (mEPSC's), tetrodotoxin (TTX) (1 μM) and bicuculline (10 μM) were added to the bath solution to block action potential dependent neurotransmitter release and GABA<sub>A</sub> channels, respectively. LTD was elicited by adding NMDA (20 μM) to the bath solution for 3 min (Carroll *et al.*, 1999b).

For slice experiments, Cal<sup>-/-</sup> and WT mice (14–49 days old) were lightly anesthetized with chloralose (10–20 mg/kg). After decapitation the brains were rapidly dissected and immersed for 1 min in cold (4°C) artificial cerebrospinal fluid (ACSF) (in mM): 200 sucrose, 1.9 KCl, 1.2 NaH<sub>2</sub>PO<sub>4</sub>, 33 NaHCO<sub>3</sub>, 0.5 CaCl<sub>2</sub>, 6 MgCl<sub>2</sub>, 10 dextrose, 0.4 ascorbic acid. Slices (300 μm) containing the hippocampal formation, were transferred to oxygenated (95% O<sub>2</sub>-5% CO<sub>2</sub>) ACSF containing (in mM): 125 NaCl, 2.5 KCl, 25 NaHCO<sub>3</sub>, 1.25 NaH<sub>2</sub>PO<sub>4</sub>, 4 MgCl<sub>2</sub>, 1 CaCl<sub>2</sub>, 0.4 ascorbic acid, 15 sucrose and 10 glucose until use. The recording solution contained (in mM): 125 NaCl, 2.5 KCl, 25 NaHCO<sub>3</sub>, 1.3 MgCl<sub>2</sub>, 2.0 CaCl<sub>2</sub>, 0.4 ascorbic acid, and 10 glucose. The slices were submerged in the recording chamber, and perfused with oxygenated recording solution at a rate of 1–3 ml/min. Pyramidal cells in CA1 were viewed using differential interference contrast (DIC) optics, and visually selected based on a smooth appearance and pyramidal shape. Whole cell patch clamp recordings were made at room temperature (25–28°C) using thick-walled borosilicate pipettes (5–8 MΩ) filled with (in mM): 125 Potassium gluconate, 20 KCl, 2 MgCl<sub>2</sub>, 10 HEPES, 1.0 EGTA, 1.0 QX-314 Cl<sup>-</sup>, 2 ATP, 0.5 GTP, 10 phosphocreatine. GST-Cal<sub>132–155</sub> or GST alone was added to the pipette solution at a final concentration of 0.6 μM with protease inhibitors leupeptin, bestatin, and pepstatin (100 μM each) where indicated. A bipolar stimulating electrode, constructed from epoxy-insulated tungsten wires, was positioned in the CA1 stratum radiatum where terminals of the Schaffer collaterals (SC) are found. Electrical stimuli consisting of low-intensity, square-wave pulses (100 μA; 100 μsec) were administered every 30 seconds in order to monitor evoked EPSC (eEPSC) amplitude over the length of the recording. The LTD induction protocol consisted of stimulating the SC for 900 pulses at 1 Hz (LFS) at same intensity as control. Baseline responses were recorded at 0.03 Hz for 10 minutes prior to delivering either control (0.03 Hz) or LFS (1.0 Hz) for 15 min. Responses were subsequently recorded at 0.03 Hz for an additional 45 min to monitor long term changes in amplitude.

Patch pipettes were connected with an Ag/AgCl wire to the headstage of a Heka EPC 9 amplifier. The EPC9 was connected to a computer running Pulse software (Heka, Lambrecht, Germany). Data was collected with a 10kHz digitization rate. An Ag/AgCl reference pellet was placed in the bath, and voltage shifts were corrected using offset. Voltage-clamp recordings were obtained in continuous single-electrode voltage-clamp mode and filtered at 1 kHz. Acceptable cells had resting potentials greater than -50 mV and input resistances greater than 40 MΩ. Series resistance was less than 12 MΩ initially and compensated 80%. Cells were discarded if series resistance increased to more than 15 MΩ

during the experiment or if there was a more than 20% change in resting potential or input resistance. Liquid junction potentials were small and not compensated. Capacitance and resistance artifacts are compensated automatically by Pulse and tuned manually. Responses were filtered at 2 Hz. Events were analyzed using MiniAnalysis program (Synaptosoft, Inc.) and the threshold for event detection was set at 5 pA. Amplitude measurements were normalized to the baseline values. The average eEPSC or mEPSC amplitude during baseline was compared to the average amplitude during the last 10 min of the recording (35–45 min after control, NMDA treatment or LFS) by Student's t-tests. The current-voltage (I–V) curves of AMPA receptor-mediated EPSCs were derived from responses recorded in the presence of D-AP5 (50  $\mu$ M) and bicuculline (50  $\mu$ M). The NMDA:AMPA ratio was calculated using the methods of Myme, et al., 2003 (Myme *et al.*, 2003). Briefly, the AMPA portion of the eEPSC was taken while holding the cell at +50 mV using the time window (1 msec) that corresponds to the peak of the response when the cell is held at –90 mV. The NMDA portion of the response was obtained by measuring the amplitude of the response in a 10 msec time window that fell 40 msec after the stimulation artifact. The ratio was calculated as follows:  $I_{\text{NMDA} + 50 \text{ mV}}/I_{\text{AMPA} + 50 \text{ mV}}$ . Additionally,  $\text{Mg}^{2+}$  was removed from the perfusion solution in order to allow clearer observation of the NMDA current.

### Cell Surface GluR1 Immunofluorescence

Hippocampal neurons (14–21 DIV) were incubated with for 30 min in ACSF (120 mM NaCl, 5 mM KCl, 5 mM HEPES, 20 mM glucose, 25 mM sucrose, 1.8 mM  $\text{CaCl}_2$ , 1.0 mM  $\text{MgCl}_2$ , 1  $\mu$ M TTX, pH7.4). Subsequently, neurons were stimulated with AMPA (100 $\mu$ M, plus 50  $\mu$ M D-AP5) or NMDA (20  $\mu$ M) both in the presence of 1  $\mu$ M TTX for 0, 5, 10, 20 min in 37  $^{\circ}$ C, or left untreated. The neurons were then fixed in 4% PFA, 4% sucrose for 5 min at RT, and blocked under non-permeabilizing conditions in blocking buffer (5% goat serum, 5% milk in PBS) at RT for 1h. Cell surface GluR1 was detected by incubating coverslips with rabbit anti-GluR1 antibody (Calbiochem, catalog number PC246) (20 $\mu$ g/ml) in blocking buffer for 2 h. After washing, coverslips were incubated with Alexa488-conjugated goat anti-rabbit secondary antibody (1:1000) in blocking buffer for 40 min. Unbound antibodies were removed by washing five times with PBS, before mounting coverslips in Prolong anti-fade medium (Invitrogen). Selective labeling of surface proteins was confirmed in parallel experiments performed on cultures blocked in permeabilizing buffer (PBS containing 5% non-fat dry milk, 5% normal goat serum (NGS) and 0.1% Triton X-100 for 1h).

Epifluorescent micrographs were taken on a Zeiss Axiovert 100 microscope using a 63X, 1.25 NA objective with a Till Photonics Imaging system that includes a Polychrome V monochromator, Imago type QE camera, and TiLL Vision software. Images for all experimental groups were taken using the identical acquisition parameters (bin setting and exposure time). GluR1 cell surface staining was quantified by the methods previously described (Beattie *et al.*, 2000; Sun *et al.*, 2005) using NIH ImageJ software (version 1.36b). Quantification was performed in a genotype and treatment blind manner. Processes located one soma diameter distance from the soma were selected for quantification, and three areas in each cell were averaged to determine the labeling of a given cell. Each group included the results of measurements performed on twenty cells. Briefly, the area (in pixels<sup>2</sup>) of fluorescence specifically corresponding to GluR1 labeling was measured using a threshold set at least two times higher than the average background fluorescence detected in comparable processes of control cells labeled with only secondary antibody. The GluR1 antibody labeled area was then normalized to the total area (in pixels<sup>2</sup>) of the labeled region by setting the threshold lower than the background fluorescence detected in control cells. Once the code was broken, values were normalized to levels detected in untreated WT

cultures, and labeling measured in three independent experiments of cultures from different litters compared the Prism 4.02 Statistics Program (GraphPad Software, Inc.).

### Biotinylation Assay of AMPA Receptor Endocytosis

Biotinylation studies were carried out following methods previously described (Ali and Bergson 2003; Ehlers 2000). Briefly, cortical neurons (14–21 DIV) plated in 60 mm dishes were pre-treated with ACSF containing 100 µg/ml leupeptin and 1 µM TTX for 30 min in 37 °C, and then incubated with 0.5 mg/ml sulfo-NHS-SS-biotin (Pierce) in PBS containing 1 mM MgCl<sub>2</sub> and 0.1 mM CaCl<sub>2</sub> for 30 min at 4°C. Unreacted biotin was quenched with three 5 min washes of ice cold 10 mM glycine in PBS on ice. After two additional washes with PBS, the neurons were treated with 20 µM NMDA plus 1 µM TTX for 0, 5 or 15min, or 20 µM NMDA plus 0.45 M sucrose for 5 or 15min at 37 °C in the presence of leupeptin. After treatment, the cells were put on ice, and the remaining surface biotin cleaved with three 20 min washes in glutathione stripping buffer (50 mM glutathione, 75 mM NaCl, 75 mM NaOH, 10% FBS) at 4°C. Cells were washed twice with PBS, and the remaining stripping buffer quenched with three 5 min washes with PBS containing 50 mM iodoacetamide plus 1% BSA. Cells were lysed, and protein concentrations determined. Sample volumes were adjusted with lysis buffer to attain equal protein concentrations in all groups. Biotinylated receptors were recovered by incubating with streptavidin agarose (Pierce) at 4°C for 2 h. Slurries were washed twice with lysis buffer, twice with 1.5 M guanidine HCl, followed by two additional washes with lysis buffer. Bound proteins were eluted with SDS loading buffer, resolved by SDS-PAGE, and immunoblotted with rabbit anti-GluR1 antibody (2 µg/ml) and HRP-conjugated secondary antibody (Jackson ImmunoResearch). Bound antibodies were detected with ECL (Amersham). Blots were stripped and re-probed with anti-GluR2 antibody (Chemicon; 1:100). Immunoblots were subjected to densitometric analysis using NIH Image J software, and band intensities normalized to untreated control values. Values obtained in three independent experiments performed on cultures from different litters were averaged, and the means ± SEM for each treatment group compared.

## Results

### Cal<sup>-/-</sup> Neurons Exhibit Alterations in Stimulated Removal of Cell Surface AMPA Receptors

Endocytosis of AMPA receptors from synapses can be triggered directly by stimulation with AMPA, or indirectly by stimulating NMDA receptors (Lee *et al.*, 1998; Carroll *et al.*, 1999a). We used an antibody recognizing an extracellular epitope of the GluR1 subunit to study the effect of the calcyon knockout on basal and activity regulated levels of endogenous AMPA receptors expressed on the cell surface of hippocampal neurons in culture (Carroll *et al.*, 1999a; Beattie *et al.*, 2000; Lin *et al.*, 2000). Immunofluorescence studies with the GluR1 antibody yielded punctate staining of fixed unpermeabilized neurons in the WT and Cal<sup>-/-</sup> cultures (fig. 1A). In contrast, an antibody directed against the cytosolic protein clathrin light chain (LC) failed to label similarly processed neurons, but robustly labeled neurons if fixed under permeabilizing conditions (data not shown). Quantification of the labeling of neuronal processes revealed no differences in GluR1 antibody staining of unstimulated WT and Cal<sup>-/-</sup> neurons (fig. 1A,B) ( $p > 0.05$ ; paired t-test).

To examine the effect of calcyon gene deletion on agonist stimulated endocytosis of AMPA receptors, WT and Cal<sup>-/-</sup> neurons were stimulated with AMPA or NMDA for up to 20 min. Reduced surface GluR1 labeling was detected in WT and Cal<sup>-/-</sup> cultures following treatment either with AMPA or NMDA. However, the effectiveness of both agonists in stimulating AMPA receptor internalization was significantly blunted in the Cal<sup>-/-</sup> neurons (fig. 1A, C, D). In contrast to basal surface levels, quantification of the immunofluorescence revealed a significant effect of genotype on agonist evoked reduction in surface GluR1

levels (genotype  $F(1, 4)=29$  and  $28$ , for AMPA and NMDA treated cells, respectively;  $p<0.01$ ). For example comparison of the time courses in three independent experiments showed that surface GluR1 labeling of WT neurons rapidly dropped to nearly 50% of basal levels with 5 min of AMPA treatment (fig. 1C). However, a much slower decrease in surface GluR1 levels was detected in the  $Cal^{-/-}$  neurons in response to AMPA where on average 80 to 90% of basal GluR1 labeling remained after 5 min of treatment. Similarly, NMDA stimulation induced a much more robust decrease in surface GluR1 levels in WT compared to  $Cal^{-/-}$  neurons (fig. 1A, D). Additionally, there was a significant interaction of time and genotype (interaction,  $F(3,12)=13$  and  $4.1$ , for AMPA ( $p<0.01$ ) and NMDA ( $p<0.05$ ), respectively) indicating that differences in the GluR1 surface levels observed in the response of the  $Cal^{-/-}$  and WT neurons to both agonists become more marked with time.

### Reduced NMDA Evoked Internalization of GluR1 and GluR2 in $Cal^{-/-}$ Neurons

We also assessed the effect of calcyon deletion on AMPA receptor endocytosis by biotinylation in neocortical neurons (Ehlers 2000). Cell surface AMPA receptors were labeled with a membrane impermeant cleavable biotin compound at  $4^{\circ}C$ . Basal cell surface GluR1 levels in the WT and  $Cal^{-/-}$  cultures were evaluated by comparing the relative amounts of receptor in the biotinylated versus lysate fractions of the untreated groups. As with the immunofluorescence data (fig. 1), this analysis showed no significant difference in cell surface levels of GluR1 in the WT and  $Cal^{-/-}$  cultures (WT vs.  $Cal^{-/-}$ ,  $28 \pm 4\%$  vs.  $37 \pm 9\%$ ,  $p>0.05$ , paired t-test) (fig. 2A, B). AMPA receptor internalization was stimulated by incubating the surface biotinylated cultures with NMDA for five or fifteen min at  $37^{\circ}C$  (fig. 2A, C). Levels of NMDA induced GluR1 internalization in the WT and  $Cal^{-/-}$  cultures were normalized to the basal surface levels detected for each genotype. Based on the average of three independent experiments, NMDA stimulated far less GluR1 internalization in the  $Cal^{-/-}$  compared to the WT neurons (genotype,  $F(1,4)=59.1$ ,  $p<0.01$ ). Indeed, two-way ANOVA comparisons revealed a strong interaction between genotype and time of NMDA treatment (interaction,  $F(2, 8)=26$ ,  $p<0.001$ ) suggesting the difference was even more pronounced with time of NMDA treatment.

Recent findings suggest that GluR2 subunits play a dominant role in the endocytosis and sorting of AMPA receptors (Lee *et al.*, 2004). To test the effect of the calcyon deletion on NMDA-stimulated GluR2 endocytosis, we re-probed the biotin blots with anti-GluR2 antibodies (fig. 2A). As noted for GluR1, NMDA stimulated internalization of GluR2 was more robust in the WT compared to the  $Cal^{-/-}$  cultures (genotype,  $F(1,4)=21.8$ ,  $p<0.01$ ), an effect that was more marked with time (interaction,  $F(2, 8)=19.2$ ,  $p<0.001$ ) (fig. 2E). In addition, no difference could be detected with respect to basal cell surface GluR2 levels in the WT and  $Cal^{-/-}$  neurons ( $p>0.05$ , paired t-test) (fig. 2D). Hypertonic sucrose abrogated the effect of NMDA on GluR1 and GluR2 internalization in both the  $Cal^{-/-}$  and WT cultures consistent with the idea that NMDA-stimulated endocytosis of AMPA receptors is clathrin mediated (Heuser and Anderson 1989) (fig. 2A). Together, the immunofluorescence and biotinylation studies support the idea that genetic deletion of calcyon impairs stimulated endocytosis of AMPA receptors. Further, since the lysosomal protease inhibitor leupeptin was included in the medium before and during the stimulation, it is unlikely that the reduced intracellular accumulation of GluR1 and GluR2 observed in the  $Cal^{-/-}$  neurons can be attributed to increased degradation (Ehlers 2000; Cottrell *et al.*, 2004).

### Basal Glutamate Transmission in CA1 is Unaltered in the Calcyon Knockout

Numerous studies indicate that vesicle trafficking of AMPA receptors in dendritic spines is important for basal neurotransmission, and also plays a key role in plasticity (Bredt and Nicoll 2003). To assess whether deletion of calcyon impacts basal glutamate transmission, we analyzed the frequency, amplitude and kinetics (rise time and decay time) of miniature

EPSCs (mEPSCs) in acute hippocampal slices (fig. 3). We analyzed an average of  $415.24 \pm 158.2$  events per WT cell ( $n=8$ ), and an average of  $442.1 \pm 151.9$  events per  $Cal^{-/-}$  cell ( $n=7$ ) were used during a 10 minute recording period. This analysis suggested that calcyon does not play a role in presynaptic glutamate release under basal conditions since the interval between events was almost identical in the knockout and WT slices ( $0.6 \pm 0.2$  Hz in  $Cal^{-/-}$ ,  $n=7$ , and  $0.5 \pm 0.3$  Hz in WT,  $n=8$ ) (fig. 3B). Consistent with this idea, the 10–90% rise time was equivalent for both genotypes ( $2.3 \pm 0.15$  msec for WT and  $2.2 \pm 0.18$  msec for  $Cal^{-/-}$ ). Additionally, decay times were also similar between the genotypes ( $9.3 \pm 0.78$  msec for WT and  $9.1 \pm 0.35$  msec for  $Cal^{-/-}$ ), suggesting that there are no differences in AMPA receptor composition. Similarly, there was no significant difference between the genotypes in the cumulative probability distribution for mEPSC amplitude, or in average raw mEPSC amplitude ( $7.1 \pm 0.4$  pA in  $Cal^{-/-}$ ,  $n=7$  and  $7.5 \pm 0.6$  pA in WT,  $n=8$ ) suggesting that basal levels of synaptic AMPA receptor conductance and/or number are similar in WT and  $Cal^{-/-}$  CA1 neurons (fig. 3C). One limitation of the results shown here involves the noise level of the recordings. With 8–10 pA of background noise, it is possible that our analysis is biased towards larger events (greater than 5 pA). Therefore, we can not rule out the possibility that calcyon deletion may affect smaller events under basal conditions.

AMPA receptor-mediated EPSCs (eEPSCs) in CA1 pyramidal neurons also showed no differences in amplitude, current/voltage relationships, or reversal potential between the WT and  $Cal^{-/-}$  slices (fig. 3D, E) again suggesting deletion of calcyon does not alter the subunit composition of synaptic AMPA receptors. Similarly, analysis of NMDA eEPSCs evoked at various membrane potentials showed that cells from  $Cal^{-/-}$  mice exhibit the characteristic J-shaped curve for NMDA I/V relationships (fig. 3E). In addition, the amplitude of NMDA responses in WT and  $Cal^{-/-}$  CA1 neurons did not differ over a range of stimulus intensities (data not shown). The NMDA:AMPA ratio was also calculated for eEPSC's (Myme *et al.*, 2003). No significant differences were detected for relative numbers of AMPA and NMDA receptors between the two genotypes (WT=0.81  $\pm$  0.04,  $n=5$ ;  $Cal^{-/-}$ =0.88  $\pm$  0.19,  $n=5$ ) (fig. 3F).

### **$Cal^{-/-}$ Neurons do not Exhibit Chemical LTD**

NMDA receptor stimulation followed by clathrin mediated endocytosis of AMPA receptors is the foundation for LTD induction and expression (Malenka and Bear 2004). Therefore, we measured synaptic activity in the  $Cal^{-/-}$  and WT cultures to determine whether the deficits in AMPA receptor endocytosis observed in the  $Cal^{-/-}$  neurons might impact synaptic plasticity. We recorded miniature excitatory synaptic currents (mEPSC's) in primary hippocampal neurons held at  $-60$  mV. Recordings were made before and after application of 20  $\mu$ M NMDA for 3 min to induce a chemical form of LTD (Lee *et al.*, 1998; Carroll *et al.*, 1999b). This protocol produced a robust ( $48 \pm 4\%$ ), persistent (lasting at least 45 min) depression of mEPSC amplitude in neurons from WT animals (fig. 4A,D;  $-13$  pA pre- vs.  $-6 \pm 0.3$  pA post-NMDA;  $n=6$ ). The reduced synaptic strength could not be attributed to long recording times or pipette solution perfusion since WT cells that did not receive NMDA but were held for the same length of time showed no change in mEPSC amplitude (fig. 4A,D;  $-10.2$  pA pre- vs.  $-10 \pm 1.3$  pA post-control;  $n=6$ ). Responses in the control  $Cal^{-/-}$  neurons also remained stable during the 1 h recording period (fig. 4B,D;  $-11$  pA pre- vs.  $-11 \pm 1.1$  pA post-control;  $n=8$ ). However, in contrast to WT, treatment of  $Cal^{-/-}$  cultures with NMDA did not produce a prolonged depression in mEPSC amplitude (fig. 4B,D;  $-12.5$  pA pre- vs.  $-12.4 \pm 1.8$  pA post-NMDA;  $n=6$ ). Interestingly, this reduction in mEPSC amplitude specifically affects larger events above 12 pA (fig. 4C). In addition, despite differences in mEPSC amplitude, there was no significant change in the frequency of mEPSC's either in the WT or  $Cal^{-/-}$  control or NMDA-treated groups (data not shown). We compared the events that occurred during the 10 minute baseline period with those in the 35

to 45 minute time window following NMDA application. The number of events analyzed per group was as follows: WT groups had an average of  $75.2 \pm 15.2$  events (baseline) or  $69.9 \pm 18.9$  events (post-NMDA), KO groups averaged  $74.5 \pm 21.6$  (baseline) or  $79.3 \pm 12.5$  (post-NMDA), The WT-GFP-Cal groups averaged  $73.9 \pm 16.8$  events (baseline) and  $75.7 \pm 15.2$  events (post-NMDA), and the KO-GFP-Cal groups averaged  $78.6 \pm 13.5$  events (baseline) or  $82.3 \pm 15.1$  events (post-NMDA). The number of mEPSC's is somewhat low compared to acute slices possibly due to reduced connectivity in the culture preparation.

### Heterologous Expression of Calcyon Rescues Chemical LTD in $Cal^{-/-}$ Cultures

To test whether the presence of calcyon is critical for the expression of AMPA receptor LTD in hippocampal neurons in culture, we transfected the cultures at 10 DIV with EGFP tagged calcyon (GFP-Cal) (fig. 4E, 4D inset), and recorded from transfected neurons. Heterologous expression of calcyon rescued the ability of the  $Cal^{-/-}$  neurons to undergo LTD as a persistent and robust ( $31 \pm 5.2\%$  below baseline) reduction in mEPSC amplitude was detected in  $Cal^{-/-}$  neurons transfected with GFP-Cal (fig. 4E,D;  $-10.5$  pA pre- vs.  $-7.3 \pm 1.9$  pA post-NMDA;  $n=6$ ). In contrast, untransfected  $Cal^{-/-}$  cells in these cultures (as evidenced by their lack of fluorescence) did not show a similar reduction in mEPSC amplitude following NMDA treatment. WT cells transfected with GFP-Cal also showed a significant reduction in mEPSC amplitude after NMDA application (fig. 4F,D;  $-11.0$  pA pre- vs.  $-8.9 \pm 1.6$  pA post-NMDA;  $n=6$ ).

### LTD is Impaired in Acute Hippocampal Slices from $Cal^{-/-}$ Mice

Since the experiments above were conducted in neurons in primary culture, we sought to determine whether calcyon deletion would have the same effect in acute brain slices. Additionally, the use of slices allowed us to induce LTD electrically, in a way that more closely mimics the repeated activity that might occur in vivo rather than a general dispersal of NMDA in the bath. We chose to examine the CA1 region of hippocampus since plasticity in this region has been extensively characterized and because calcyon is abundantly expressed in rodent CA1 (Zelenin *et al.*, 2002). We recorded evoked EPSCs (eEPSCs) in CA1 of acute hippocampal slices from WT and  $Cal^{-/-}$  animals following extracellular stimulation in the Schaffer collaterals (SC). Cells were maintained at a constant holding potential of  $-60$  mV. Baseline measurements were elicited by stimulating at a frequency of 0.03 Hz, and eEPSC amplitude was monitored for at least 20 min. Once the amplitude stabilized (typically 10–15 minutes after breaking into the cell) and baseline measurements were obtained, LTD was induced by stimulating ( $100 \mu A$ ) in the SC at a frequency of 1 Hz for 900 pulses (LFS) or 15 min. Control cells in each group were stimulated at the baseline frequency (0.03 Hz) for 15 min. All cells were held and monitored for an additional 45 min in order to measure long term changes in eEPSC amplitude.

Figure 5A shows the normalized change in eEPSC amplitude from baseline (set to 0%) over time for CA1 neurons in WT slices in response to LFS (open circles), or the control stimulation protocol of 0.03 Hz (filled squares). WT cells receiving the 1 Hz stimulation exhibited a significant decrease in synaptic strength (fig. 5A;  $n=8$ ), whereas control cells held for a similar period of time did not show differences in average eEPSC amplitude over time (control ( $n=8$ ),  $2.8 \pm 1.5\%$  versus LFS,  $-45.3 \pm 2.8\%$ ). Also, the differences observed in the LFS stimulated cells could not be attributed to changes in the series resistance or differences in cell health since holding potential remained constant throughout the recordings.

Bar graphs in fig. 5D show the differences between the two groups (control and LFS) during the last 10 minutes of the recording. In contrast to the  $58 \pm 2\%$  decrease detected in WT slices, LFS did *not* evoke a persistent decrease in eEPSC amplitude in CA1 neurons of slices



prepared from  $Cal^{-/-}$  mice (fig. 5B, D; n=8). Despite the genotypic differences in the prolonged effects of LFS on eEPSC amplitude, the responses were equally depressed during LFS in WT ( $-98.2 \pm 21.6\%$ ) and KO ( $-99.2 \pm 17.1\%$ ) cells. Further, as with the WT neurons, the control stimulation protocol did not produce significant changes in the average eEPSC amplitude over time in the KO neurons (control  $-3.2\% \pm 1.3\%$ , LFS  $-4.14 \pm 3.2\%$ ).

### The Role of Calcyon in LTD Involves Interaction with Clathrin LC

Deletion of calcyon did not appear to grossly alter synaptic activity or basic cellular characteristics of the CA1 neurons since eEPSCs during baseline stimulation of the  $Cal^{-/-}$  slices were similar in size ( $52.9 \pm 3.6$  pA; n=8) to the WT responses ( $54.9 \pm 2.3$  pA; n=8) (fig. 5F). Additionally, input resistance values of the  $Cal^{-/-}$  CA1 neurons ( $166.2 \pm 12.2$  M $\Omega$ ; n=8) were similar to what was measured in WT slices ( $154.2 \pm 12.9$  M $\Omega$ ; n=8). Further, the holding current required to maintain  $Cal^{-/-}$  and WT cells at  $-60$  mV were similar. Given that the response to the baseline stimulus remained relatively constant over the length of the recording, the absence of LTD in the  $Cal^{-/-}$  slices following LFS is consistent with defects in clathrin mediated endocytosis of synaptic AMPA receptors.

Previous analyses indicate the interaction of clathrin LC and calcyon involves sequences in the carboxy terminal cytoplasmic segment of calcyon (Xiao *et al.*, 2006). The LC binding region in calcyon was pared down in pull-down experiments with a set of glutathione-S-transferase (GST) constructs including N- and C-terminal deletions of the calcyon C-terminus (114–217) (fig. 6). Equimolar amounts of each GST calcyon deletion construct were pre-bound to glutathione resin and tested for the ability to retain full length S-Tag-LC (S-LC). One construct, GST- $Cal_{123-155}$  exhibited binding to S-LC comparable to that obtained with GST- $Cal_{114-217}$ , indicating residues 123 to 155 likely include sequences required for binding LC.

We used GST- $Cal_{123-155}$  to further probe the mechanism underlying the defects in LTD detected in  $Cal^{-/-}$  CA1 neurons. We hypothesized that blocking the interaction of calcyon with LC by intracellular perfusion of the calcyon LC binding domain might prevent the ability of WT CA1 neurons to undergo LTD. Protease inhibitors were also included in the patch pipette in order to ensure that there would be no degradation of GST or the GST- $Cal_{123-155}$  fusion protein. The bar graphs in fig. 5D show the change in eEPSC amplitude after control or LFS in WT slices (last 10 minutes of recording is compared to baseline measurement) where the LC binding domain of calcyon (GST- $Cal_{123-155}$ ;  $0.6$   $\mu$ M), or control protein (GST;  $0.6$   $\mu$ M) were added to the recording pipette. As shown in fig. 5C,D, LTD could not be detected following LFS of WT CA1 neurons perfused with GST- $Cal_{123-155}$  via the patch pipette ( $-1.59 \pm 7.65\%$  change, n=5). In contrast, inclusion of GST protein alone in the patch pipette did not impair the ability of WT CA1 neurons to undergo LTD in response to LFS ( $-71.22 \pm 5.7\%$  change, n=4). These data suggested that interaction of calcyon with clathrin LC plays an important role in activity regulated clathrin mediated endocytosis of synaptic AMPA receptors.

## Discussion

The studies presented above indicate that calcyon regulates activity-dependent clathrin mediated endocytosis of postsynaptic AMPA receptors, and NMDA-dependent LTD. Previous studies suggest that calcyon stimulates clathrin coated vesicle (CCV) assembly in vitro and CME in vivo (Xiao *et al.*, 2006). Hence, a possible explanation for the present findings is that calcyon facilitates removal of a sufficient number of postsynaptic AMPA receptors for LTD by regulating CCV formation. Presynaptic mechanisms involving alterations in release probability are also implicated in NMDA receptor dependent LTD

(Zhang *et al.*, 2005). However, the observation that the frequency of mEPSCs is similar in the Cal<sup>-/-</sup> and WT neurons before and after LTD induction argues against a presynaptic explanation for the lack of LTD in the calcyon knockout. Additionally, the ability of knockout neurons to undergo LTD when transfected with GFP-Calcyon is consistent with a postsynaptic mechanism since mEPSC amplitude was decreased but there was no change in frequency, similar to what was observed in WT cultures. The GFP-Calcyon rescue studies further suggest that the LTD deficiency in the knockout does not arise from a compensatory response to the absence of calcyon.

AMPA receptors undergo two types of clathrin mediated endocytosis, stimulated and constitutive (Sheng and Hyoun 2003). Our data suggests that calcyon regulates stimulated endocytosis of synaptic AMPA receptors since LTD was abolished, and AMPA and/or NMDA-evoked internalization of GluR1 and GluR2 was significantly reduced in knockout neurons. Indeed, the levels of agonist stimulated GluR1 and GluR2 surface levels and/or internalization that we detected in WT neuronal cultures corresponded well those reported in earlier studies of endogenous AMPARs in comparable neuronal culture systems (Lin *et al.*, 2000; Ehlers 2000). For example, despite differences in immunodetection methods, we found that AMPA exerted a comparable effect on the time constant ( $\tau$ ) for the rate of reduction in surface GluR1 ( $\tau = 3.88$  min, our study) in WT neurons as previously reported for the rate of surface GluR1 internalization ( $\tau = 3.1$ ) (Lin *et al.*, 2000). Similarly, our measurements of NMDA stimulated GluRs internalization by biotinylation of WT cultures are in line with those reported by Ehlers (2000), taking into consideration that after 10 min of NMDA treatment, the levels of internalized GluRs are depleted as a result of recycling to the cell surface. Indeed, earlier studies indicate that effects observed at 5 min time points for the most part reflect AMPAR endocytosis, with little or no contribution from recycling (Ehlers 2000; Lin *et al.*, 2000). If this assumption is valid, the differences detected in the WT and Cal<sup>-/-</sup> samples at 5 min in both the immunofluorescence and biotin studies would indicate that, in the presence of agonist, calcyon *facilitates* endocytosis of GluR1 and GluR2 by a factor of two to three. Overall, the similarities in the effects of agonists on GluR surface levels and internalization in WT cultures with previous studies (Ehlers 2000; Lin *et al.*, 2000) validate our findings, whereas the alterations detected in Cal<sup>-/-</sup> cultures suggest calcyon plays an important role in regulating stimulated endocytosis of postsynaptic AMPARs.

When combined with tetrodotoxin as in our biotinylation and immunofluorescence studies, previous studies suggest that NMDA and AMPA have different effects on AMPA receptor cycling with AMPA favoring sorting to lysosomes, and NMDA promoting recycling to the plasma membrane (Lin *et al.*, 2000; Ehlers, 2000; Lee *et al.*, 2004). We found that the effect of deleting calcyon on internalization of receptors destined for either endocytic pathway was equally dramatic. Therefore, our data would suggest that calcyon might act upstream of the recycling/degradation decision proposed to occur at the CCV assembly stage (Lakadamyali *et al.*, 2006).

If calcyon also regulates GluR constitutive endocytosis, one might expect to find higher GluR surface levels in the knockout cultures, or an increase in mEPSC amplitude or frequency due to basal recycling of GluR subunits into synapses (Luscher *et al.*, 1999; Noel *et al.*, 1999). Instead, we found that AMPA component of evoked and miniature EPSC amplitude under basal conditions did not significantly differ between Cal<sup>-/-</sup> and WT neurons. Notably, these events primarily reflect *synaptic* AMPA channels because of the relatively low affinity of GluRs for glutamate and the depolarization requirement of NMDA receptors. Thus, the similarity in amplitude, rise time, decay time, frequency of events (IEI), as well as the similarity in AMPA I-V curves between knockout and WT slices suggests that under basal conditions synaptic AMPA receptor number and composition are unaffected by knockout of calcyon. Further, the similarity of the AMPA current rectification index

obtained for WT and Cal<sup>-/-</sup> neurons indicated that knockout of calcyon does not effect synaptic AMPA receptor subunit composition. Consistent with the electrophysiological recordings, our immunofluorescence and biotin studies revealed no effect of the calcyon deletion on basal surface GluR1 or GluR2 levels. Taken together, the present data suggests that calcyon does not appreciably regulate endocytosis of synaptic AMPA receptors during conditions of basal synaptic transmission. However, it is important to note that our studies did not directly address whether knockout of calcyon might significantly alter *rates* of GluR basal endocytosis. Therefore, the apparent lack of effect on basal endocytosis could involve a reduction in the basal rate of AMPA receptor recycling via a homeostatic mechanism to maintain levels of synaptic transmission (Man *et al.*, 2000). Alternatively, calcyon might also regulate basal GluR recycling. Additionally, it has been proposed that basal exchange of surface and intracellular receptors occurs largely at extrasynaptic sites (Adesnik *et al.*, 2005). If calcyon primarily regulates endocytosis of synaptic receptors, such an effect might not be detected. Consistent with this possibility, the present studies were conducted in mature (14 to 21 DIV) neurons in culture where approximately 75 to 80% of endogenous GluR1 and GluR2 subunits expressed on the surface are synaptic (Passafaro *et al.*, 2001).

A number of other clathrin adaptor and accessory proteins have previously been shown to regulate GluR internalization and LTD in CA1 neurons (Luscher *et al.*, 1999;Carroll *et al.*, 1999a;Rial Verde *et al.*, 2006;Chowdhury *et al.*, 2006;Lee *et al.*, 2002;Kastning *et al.*, 2007;Palmer *et al.*, 2005). Endocytic adaptor proteins such as AP2 function by binding cargo and membrane lipids, or stabilizing interactions between legs of the clathrin heavy chain (HC) triskelions, while other accessory proteins such as endophilin, dynamin, and synaptojanin are required, respectively, for membrane deformation, scission, and uncoating of the lattice coated vesicle (Brodsky *et al.*, 2001). To our knowledge calcyon is the first *transmembrane* protein identified thus far that regulates clathrin-mediated endocytosis of postsynaptic AMPARs. Previous studies showed that calcyon stimulates CCV assembly in vitro, presumably by interacting with the C-terminus and heavy chain binding domains of clathrin light chain (LC). The role of clathrin LC in CCV formation is not well understood. Indeed, LC is apparently not an obligate subunit for clathrin mediated endocytosis in non-neuronal cells where it is typically much less abundant than in brain (Huang *et al.*, 2004;Girard *et al.*, 2005). However, in brain LC to HC exist in a one to one stoichiometry (Girard *et al.*, 2005). At this stoichiometry, LC would be predicted to negatively regulate clathrin lattice assembly and disrupt assembled cages (Ungewickell and Ungewickell 1991). Our data suggests that the LC/calcyon interaction is critical for expression of LTD since addition of the LC binding domain of calcyon (GST-Cal<sub>123-155</sub>) to the recording pipette interferes with LTD expression in WT cells, an effect that was not detected in WT cells perfused with and equivalent concentration of GST only. As clathrin HC also binds to the region of clathrin LC that interacts with calcyon (Brodsky *et al.*, 2001), one possibility is that GST-Cal<sub>123-155</sub> depletes levels of LC available for interaction with HC, or interferes with the interaction of another as yet uncharacterized protein that binds the same region of calcyon. Further, by directly binding LC, calcyon can presumably influence the localization of LC. Hence, the ability of GST-Cal<sub>123-155</sub> to block induction of LTD might result from mis-localization of LC with respect to the 'endocytic zone.' If LC is essential for increasing the rate of CCV formation, or disassembly and reassembly, during agonist or low frequency stimulation, mislocalization of clathrin LC resulting from calcyon over-expression could potentially also explain the reduced level of LTD detected in WT cultures transfected with GFP-calcyon. Alternatively, previous work in CA1 hippocampal slices showed that increased LTD magnitude is correlated with reduced basal activity (Zhang *et al.*, 2005). As the untransfected cultures were plated at a lower density than the GFP-Cal transfected cultures, it is possible that the untransfected cultures behave in a similar manner, with decreased basal activity that might change the characteristics of LTD.

High levels of the calcyon LC binding domain as in the fusion protein perfused cells might also disrupt TGN trafficking since vesicle trafficking from TGN to endosomes, and endosomes to lysosome can be clathrin mediated (Bonifacino and Lippincott-Schwartz 2003). While the current data can not exclude a role for calcyon in the post-endocytic sorting of internalized AMPA receptors, both the time course as well as the 'direction' of our data would seem to more strongly suggest a primary effect on endocytosis. This view is based on studies of rates of plasma membrane insertion of *endogenous* synaptic and extrasynaptic AMPA receptors presented in Adesnik et al., (2005) where it was estimated that exchange of synaptic AMPARs is slow (e.g., 25% in 3 h) and extrasynaptic is much faster (e.g., 35% in 30 min). As synaptic AMPARs are the main contributors to the evoked or spontaneous currents detected, based on their slow exchange time, a solely exocytic trafficking-based explanation for the data seems less likely since a typical cell perfusion experiment might last only 75 to 90 min. Also, if the key causal factor in the phenotype was disrupted trafficking of intracellular AMPARs from the TGN to endosomes en route to the plasma membrane (extrasynaptic or synaptic), one would expect to observe more severe LTD in the GST-Cal123–155 perfused neurons. On the contrary, we detected greatly reduced LTD in these cells.

It is interesting to note that stimulated AMPAR endocytosis is also impaired in knockouts of another clathrin LC interacting protein, huntingtin interacting protein 1 (Hip1) (Metzler *et al.*, 2001). As both calcyon and Hip1 stimulated assembly in vitro (Xiao *et al.*, 2006; Chen and Brodsky 2005), the Hip1 knockout and present data on calcyon raise the possibility clathrin LC plays a pivotal role in activity stimulated endocytosis of postsynaptic AMPARs. It is unclear why deletions of clathrin LC interacting proteins such as calcyon and Hip1 manifest as defects in stimulated endocytosis, whereas alterations in AP2 or endophilin interactions also impact basal transmission and GluR surface levels (Kastning *et al.*, 2007; Chowdhury *et al.*, 2006). One possibility is that  $Ca^{++}$  plays a role since synaptic activity and NMDA-evoked LTD, as well as AMPA stimulated GluR internalization are all  $Ca^{++}$  dependent events (Lin *et al.*, 2000; Malenka and Bear 2004).  $Ca^{++}$  regulates rates of exchange of HC bound and HC free clathrin LC, a process implicated the dynamic expansion of the clathrin lattice that occurs during the formation of a spherical CCV from a planar clathrin coated pit (Wu *et al.*, 2001; Loerke *et al.*, 2005). Additionally, there are indications from real time imaging studies that LC levels near synapses may be insufficient to support CCV formation during periods of rapid neuronal firing (Mueller *et al.*, 2004). Since elevated intracellular  $Ca^{++}$  levels stimulate translocation of calcyon to the plasma membrane in heterologous cells (Ali and Bergson 2003), future studies could clarify whether calcyon might also function to recruit LC to sites of endocytosis, or perhaps define novel or additional sites of endocytosis.

Altogether the present work highlights a central function of calcyon in glutamate transmission and LTD. As knockdown of the closely related protein NEEP21 impairs GluR recycling into synapses and LTP (Alberi *et al.*, 2005), it appears that the calcyon/NEEP21 protein family performs vesicle trafficking-related functions important for synaptic plasticity. Future studies might address whether the related protein, P19, also plays a role in synaptic plasticity (Saberan-Djoneidi *et al.*, 1995).

## Acknowledgments

This work was supported by NIH R01 MH63271 (CB), P50 MH068789 (McCormick, PI, Co-PI Project 1, CB), and Neuroscience Training Grant T32 NS045543 (HTD). We thank our colleagues Nevin Lambert, Almira Vazdarjanova and Sergei Kirov (Medical College of Georgia), Lynn Selemon (Yale University) and Robert Levenson (Penn State College of Medicine), for helpful comments and suggestions.

## Abbreviations

<b>LTD</b>	long-term potentiation
<b>LTP</b>	long-term depression
<b>CME</b>	clathrin mediated endocytosis
<b>CCV</b>	clathrin coated vesicle
<b>AMPA</b>	$\alpha$ -amino-3-hydroxy-5-methyl-4-isoxazolepropionic acid receptors
<b>NMDA</b>	N-methyl-D-aspartate
<b>KO</b>	knockout

## Reference List

- Adesnik H, Nicoll RA, England PM. Photoinactivation of native AMPA receptors reveals their real-time trafficking. *Neuron*. 2005; 48:977–985. [PubMed: 16364901]
- Alberi S, Boda B, Steiner P, Nikonenko I, Hirling H, Muller D. The endosomal protein NEEP21 regulates AMPA receptor-mediated synaptic transmission and plasticity in the hippocampus. *Mol Cell Neurosci*. 2005; 29:313–319. [PubMed: 15911354]
- Ali MK, Bergson C. Elevated intracellular calcium triggers recruitment of the receptor cross-talk accessory protein calcyon to the plasma membrane. *J Biol Chem*. 2003; 278:51654–51663. [PubMed: 14534309]
- Beattie EC, Carroll RC, Yu X, Morishita W, Yasuda H, von Zastrow M, Malenka RC. Regulation of AMPA receptor endocytosis by a signaling mechanism shared with LTD. *Nat Neurosci*. 2000; 3:1291–1300. [PubMed: 11100150]
- Bonifacino JS, Lippincott-Schwartz J. Coat proteins: shaping membrane transport. *Nat Rev Mol Cell Biol*. 2003; 4:409–414. [PubMed: 12728274]
- Bredt DS, Nicoll RA. AMPA receptor trafficking at excitatory synapses. *Neuron*. 2003; 40:361–379. [PubMed: 14556714]
- Brodsky FM, Chen CY, Knuehl C, Towler MC, Wakeham DE. Biological basket weaving: formation and function of clathrin-coated vesicles. *Annu Rev Cell Dev Biol*. 2001; 17:517–568. [PubMed: 11687498]
- Brown TC, Tran IC, Backos DS, Esteban JA. NMDA receptor-dependent activation of the small GTPase Rab5 drives the removal of synaptic AMPA receptors during hippocampal LTD. *Neuron*. 2005; 45:81–94. [PubMed: 15629704]
- Carroll RC, Beattie EC, Xia H, Luscher C, Altschuler Y, Nicoll RA, Malenka RC, von Zastrow M. Dynamin-dependent endocytosis of ionotropic glutamate receptors. *Proc Natl Acad Sci USA*. 1999a; 96:14112–14117. [PubMed: 10570207]
- Carroll RC, Lissin DV, von Zastrow M, Nicoll RA, Malenka RC. Rapid redistribution of glutamate receptors contributes to long-term depression in hippocampal cultures. *Nat Neurosci*. 1999b; 2:454–460. [PubMed: 10321250]
- Chen CY, Brodsky FM. Huntingtin-interacting protein 1 (Hip1) and Hip1-related protein (Hip1R) bind the conserved sequence of clathrin light chains and thereby influence clathrin assembly in vitro and actin distribution in vivo. *J Biol Chem*. 2005; 280:6109–6117. [PubMed: 15533940]
- Chowdhury S, Shepherd JD, Okuno H, Lyford G, Petralia RS, Plath N, Kuhl D, Hagan RL, Worley PF. Arc/Arg3.1 interacts with the endocytic machinery to regulate AMPA receptor trafficking. *Neuron*. 2006; 52:445–459. [PubMed: 17088211]
- Cottrell JR, Borok E, Horvath TL, Nedivi E. CPG2: a brain- and synapse-specific protein that regulates the endocytosis of glutamate receptors. *Neuron*. 2004; 44:677–690. [PubMed: 15541315]
- Ehlers MD. Reinsertion or degradation of AMPA receptors determined by activity-dependent endocytic sorting. *Neuron*. 2000; 28:511–525. [PubMed: 11144360]

- Girard M, Allaire PD, McPherson PS, Blondeau F. Non-stoichiometric relationship between clathrin heavy and light chains revealed by quantitative comparative proteomics of clathrin-coated vesicles from brain and liver. *Mol Cell Proteomics*. 2005; 4:1145–1154. [PubMed: 15933375]
- Heuser JE, Anderson RG. Hypertonic media inhibit receptor-mediated endocytosis by blocking clathrin-coated pit formation. *J Cell Biol*. 1989; 108:389–400. [PubMed: 2563728]
- Huang F, Khvorova A, Marshall W, Sorkin A. Analysis of clathrin-mediated endocytosis of epidermal growth factor receptor by RNA interference. *J Biol Chem*. 2004; 279:16657–16661. [PubMed: 14985334]
- Itto M. Long-term depression. *Annu Rev Neurosci*. 1989; 12:85–102. [PubMed: 2648961]
- Kastning K, Kukhtina V, Kittler JT, Chen G, Pechstein A, Enders S, Lee SH, Sheng M, Yan Z, Haucke V. Molecular determinants for the interaction between AMPA receptors and the clathrin adaptor complex AP-2. *Proc Natl Acad Sci USA*. 2007; 104:2991–2996. [PubMed: 17289840]
- Kesner RP, Rolls ET. Role of long-term synaptic modification in short-term memory. *Hippocampus*. 2001; 11:240–250. [PubMed: 11769307]
- Lakadamyali M, Rust MJ, Zhuang X. Ligands for clathrin-mediated endocytosis are differentially sorted into distinct populations of early endosomes. *Cell*. 2006; 124:997–1009. [PubMed: 16530046]
- Lee HK, Kameyama K, Huganir RL, Bear MF. NMDA induces long-term synaptic depression and dephosphorylation of the GluR1 subunit of AMPA receptors in hippocampus. *Neuron*. 1998; 21:1151–1162. [PubMed: 9856470]
- Lee SH, Liu L, Wang YT, Sheng M. Clathrin adaptor AP2 and NSF interact with overlapping sites of GluR2 and play distinct roles in AMPA receptor trafficking and hippocampal LTD. *Neuron*. 2002; 36:661–674. [PubMed: 12441055]
- Lee SH, Simonetta A, Sheng M. Subunit rules governing the sorting of internalized AMPA receptors in hippocampal neurons. *Neuron*. 2004; 43:221–236. [PubMed: 15260958]
- Lin JW, Ju W, Foster K, Lee SH, Ahmadian G, Wyszynski M, Wang YT, Sheng M. Distinct molecular mechanisms and divergent endocytotic pathways of AMPA receptor internalization. *Nat Neurosci*. 2000; 3:1282–1290. [PubMed: 11100149]
- Loerke D, Wienisch M, Kochubey O, Klingauf J. Differential control of clathrin subunit dynamics measured with EW-FRAP microscopy. *Traffic*. 2005; 6:918–929. [PubMed: 16138905]
- Luscher C, Xia H, Beattie EC, Carroll RC, von Zastrow M, Malenka RC, Nicoll RA. Role of AMPA receptor cycling in synaptic transmission and plasticity. *Neuron*. 1999; 24:649–658. [PubMed: 10595516]
- Lynch G, Baudry M. The biochemistry of memory: a new and specific hypothesis. *Science*. 1984; 224:1057–1063. [PubMed: 6144182]
- Malenka RC, Bear MF. LTP and LTD: an embarrassment of riches. *Neuron*. 2004; 44:5–21. [PubMed: 15450156]
- Malinow R. AMPA receptor trafficking and long-term potentiation. *Philos Trans R Soc Lond B Biol Sci*. 2003; 358:707–714. [PubMed: 12740116]
- Man HY, Lin JW, Ju WH, Ahmadian G, Liu L, Becker LE, Sheng M, Wang YT. Regulation of AMPA receptor-mediated synaptic transmission by clathrin-dependent receptor internalization. *Neuron*. 2000; 25:649–662. [PubMed: 10774732]
- Metzler M, Legendre-Guillemin V, Gan L, Chopra V, Kwok A, McPherson PS, Hayden MR. HIP1 functions in clathrin-mediated endocytosis through binding to clathrin and adaptor protein. *J Biol Chem*. 2001; 276:39271–39276. [PubMed: 11517213]
- Mueller VJ, Wienisch M, Nehring RB, Klingauf J. Monitoring clathrin-mediated endocytosis during synaptic activity. *J Neurosci*. 2004; 24:2004–2012. [PubMed: 14985443]
- Myme CI, Sugino K, Turrigiano GG, Nelson SB. The NMDA-to-AMPA ratio at synapses onto layer 2/3 pyramidal neurons is conserved across prefrontal and visual cortices. *J Neurophysiol*. 2003; 90:771–779. [PubMed: 12672778]
- Noel J, Ralph GS, Pickard L, Williams J, Molnar E, Uney JB, Collingridge GL, Henley JM. Surface expression of AMPA receptors in hippocampal neurons is regulated by an NSF-dependent mechanism. *Neuron*. 1999; 23:365–376. [PubMed: 10399941]

- Oakman SA, Meador-Woodruff JH. Calcyon transcript expression in macaque brain. *J Comp Neurol.* 2004; 468:264–276. [PubMed: 14648684]
- Palmer CL, Lim W, Hastie PG, Toward M, Korolchuk VI, Burbidge SA, Banting G, Collingridge GL, Isaac JT, Henley JM. Hippocalcin functions as a calcium sensor in hippocampal LTD. *Neuron.* 2005; 47:487–494. [PubMed: 16102532]
- Park M, Penick EC, Edwards JG, Kauer JA, Ehlers MD. Recycling endosomes supply AMPA receptors for LTP. *Science.* 2004; 305:1972–1975. [PubMed: 15448273]
- Passafaro M, Piech V, Sheng M. Subunit-specific temporal and spatial patterns of AMPA receptor exocytosis in hippocampal neurons. *Nat Neurosci.* 2001; 4:917–926. [PubMed: 11528423]
- Redmond L, Kashani AH, Ghosh A. Calcium regulation of dendritic growth via CaM kinase IV and CREB-mediated transcription. *Neuron.* 2002; 34:999–1010. [PubMed: 12086646]
- Rial Verde EM, Lee-Osbourne J, Worley PF, Malinow R, Cline HT. Increased expression of the immediate-early gene *arc/arg3.1* reduces AMPA receptor-mediated synaptic transmission. *Neuron.* 2006; 52:461–474. [PubMed: 17088212]
- Sabaran-Djoneidi D, Marey-Semper I, Picart R, Studler JM, Tougard C, Glowinski J, Levi-Strauss M. A 19-kDa protein belonging to a new family is expressed in the Golgi apparatus of neural cells. *J Biol Chem.* 1995; 270:1888–1893. [PubMed: 7829526]
- Sabaran-Djoneidi D, Picart R, Escalier D, Gelman M, Barret A, Tougard C, Glowinski J, Levi-Strauss M. A 21-kDa polypeptide belonging to a new family of proteins is expressed in the Golgi apparatus of neural and germ cells. *J Biol Chem.* 1998; 273:3909–3914. [PubMed: 9461575]
- Sheng M, Hyoung LS. AMPA receptor trafficking and synaptic plasticity: major unanswered questions. *Neurosci Res.* 2003; 46:127–134. [PubMed: 12767475]
- Shi S, Hayashi Y, Esteban JA, Malinow R. Subunit-specific rules governing AMPA receptor trafficking to synapses in hippocampal pyramidal neurons. *Cell.* 2001; 105:331–343. [PubMed: 11348590]
- Steiner P, Alberi S, Kulangara K, Yersin A, Sarria JC, Regulier E, Kasas S, Dietler G, Muller D, Catsicas S, Hirling H. Interactions between NEEP21, GRIP1 and GluR2 regulate sorting and recycling of the glutamate receptor subunit GluR2. *EMBO J.* 2005; 24:2873–2884. [PubMed: 16037816]
- Steiner P, Sarria JC, Glauser L, Magnin S, Catsicas S, Hirling H. Modulation of receptor cycling by neuron-enriched endosomal protein of 21 kD. *J Cell Biol.* 2002; 157:1197–1209. [PubMed: 12070131]
- Sun X, Zhao Y, Wolf ME. Dopamine receptor stimulation modulates AMPA receptor synaptic insertion in prefrontal cortex neurons. *J Neurosci.* 2005; 25:7342–7351. [PubMed: 16093384]
- Teyler TJ, Discenna P. Long-term potentiation as a candidate mnemonic device. *Brain Res.* 1984; 319:15–28. [PubMed: 6324959]
- Ungewickell E, Ungewickell H. Bovine brain clathrin light chains impede heavy chain assembly in vitro. *J Biol Chem.* 1991; 266:12710–12714. [PubMed: 2061336]
- Wang YT, Linden DJ. Expression of cerebellar long-term depression requires postsynaptic clathrin-mediated endocytosis. *Neuron.* 2000; 25:635–647. [PubMed: 10774731]
- Wenthold RJ, Petralia RS, Blahos J II, Niedzielski AS. Evidence for multiple AMPA receptor complexes in hippocampal CA1/CA2 neurons. *J Neurosci.* 1996; 16:1982–1989. [PubMed: 8604042]
- Wu X, Zhao X, Baylor L, Kaushal S, Eisenberg E, Greene LE. Clathrin exchange during clathrin-mediated endocytosis. *J Cell Biol.* 2001; 155:291–300. [PubMed: 11604424]
- Xiao J, Dai R, Negyessy L, Bergson C. Calcyon, a novel partner of clathrin light chain, stimulates clathrin-mediated endocytosis. *J Biol Chem.* 2006; 281:15182–15193. [PubMed: 16595675]
- Zelenin S, Aperia A, Diaz HR. Calcyon in the rat brain: cloning of cDNA and expression of mRNA. *J Comp Neurol.* 2002; 446:37–45. [PubMed: 11920718]
- Zhang J, Yang Y, Li H, Cao J, Xu L. Amplitude/frequency of spontaneous mEPSC correlates to the degree of long-term depression in the CA1 region of the hippocampal slice. *Brain Res.* 2005; 1050:110–117. [PubMed: 15978556]

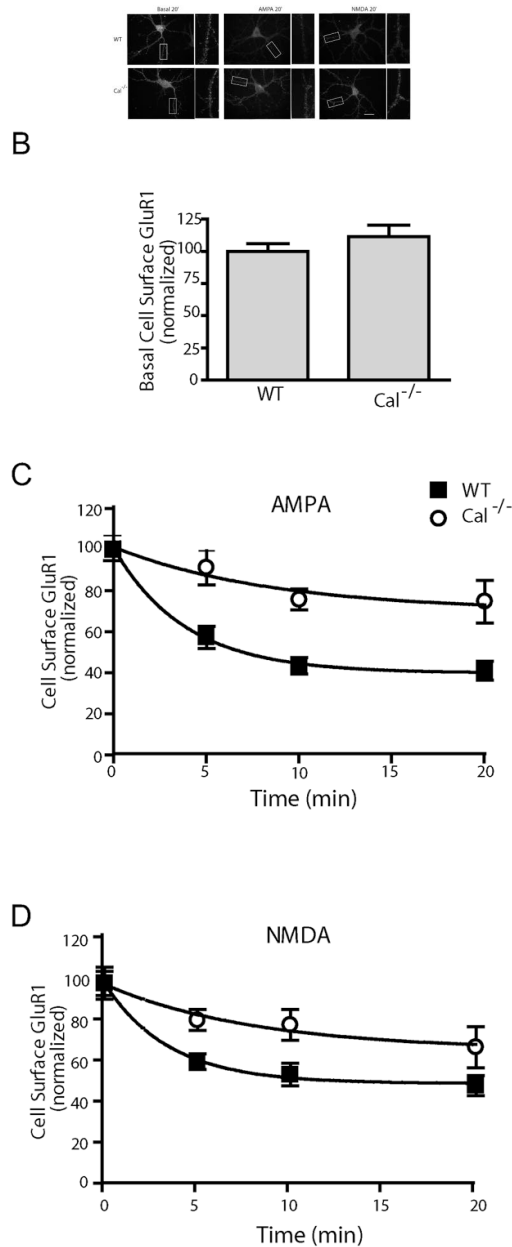


**Figure 1. AMPA and NMDA induced AMPA receptor internalization is impaired in Calcyon knockout hippocampal neurons**

(A) Neurons (14–21 DIV) from WT or calcyon knock out (Cal<sup>-/-</sup>) mice were treated at 37°C with 100μM AMPA + 50 μM D-AP5 (AMPA), 20 μM NMDA (NMDA), or left untreated as described in the Methods for the times indicated. Cell surface GluR1s were detected by immunofluorescence in fixed, non-permeabilized cells, and normalized to levels detected in untreated WT neurons. (B) Bar graph showing the mean and error bars the SEM for the cell surface GluR1 antibody staining detected in untreated WT (n=26) and Cal<sup>-/-</sup> (n=33) neurons. (C,D) The response cell surface GluR1 staining detected following 5, 10 and 20 min of AMPA (C) or NMDA (D) treatment in WT (filled squares) and Cal<sup>-/-</sup> (open circles) neurons. While no differences were detected in GluR1 surface levels in untreated neurons ( $p>0.05$ , paired t-test), deletion of calcyon significantly slowed agonist stimulated reduction in GluR1 surface levels (genotype F(1, 4)=29 and 28, for AMPA and NMDA



treated cells, respectively;  $p < 0.01$ ). Statistics are based on results obtained in three independent experiments, and results of a representative experiment are shown.

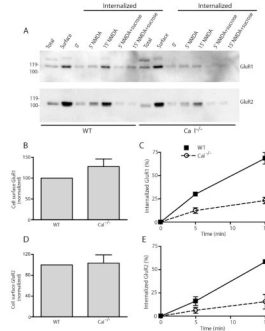


**Figure 2. Knockout of calcyon inhibits NMDA-induced AMPA receptor internalization**  
 (A) WT and  $Ca^{2+/-}$  neocortical neurons (14–21 DIV) were pre-labeled with cell-impermeant, sulfo-NHS-SS-biotin on ice. Subsequently, cultures were shifted to 37°C, and treated with NMDA (20  $\mu$ M + TTX), or NMDA in hypertonic sucrose for 5 or 15 min. Biotinylated proteins remaining on the cell surface of all drug treated groups were stripped with glutathione. To detect basal surface levels of GluR1 (Surface) before drug treatment, neurons were maintained on ice for 15 min and not stripped with glutathione. Biotinylated receptors were recovered from lysates (500  $\mu$ g) with streptavidin agarose. Total (5% of the lysates) and resin-eluted proteins (60% of each sample) were immunoblotted with rabbit anti-GluR1 or mouse anti-GluR2 antibodies. Immunoblots were subjected to densitometric analysis using NIH Image J software. The blots shown are representative of the results obtained in each of three independent experiments. Cell surface GluR1 (B) or GluR2 (D) levels in the WT and  $Ca^{2+/-}$  cultures were determined by normalizing the intensity of the cell surface bands to those of the lysates, and correcting for differences in sample loading. Bar graphs show the mean, and error bars the SEM of three independent experiments performed on different cell culture preparations. No significant differences were detected for either GluR1 and GluR2 surface levels ( $p > 0.05$ , t-test). Average time course of GluR1 (C) and GluR2 (E) internalization in WT (filled squares) and  $Ca^{2+/-}$  (open circles) cultures calculated from the ratio of the band intensities in the treated lanes at 5 and 15 min with that of the cell surface lanes (error bars indicate the SEM) of three independent experiments. Agonist stimulated internalization of both GluR1 and GluR2 significantly differed in WT and  $Ca^{2+/-}$  neurons (genotype,  $F(1,4)=59.1$  and  $21.8$ , for GluR1 and GluR2, respectively,  $p < 0.01$ ) suggesting deletion of calcyon strongly impacts agonist dependent AMPA receptor endocytosis.

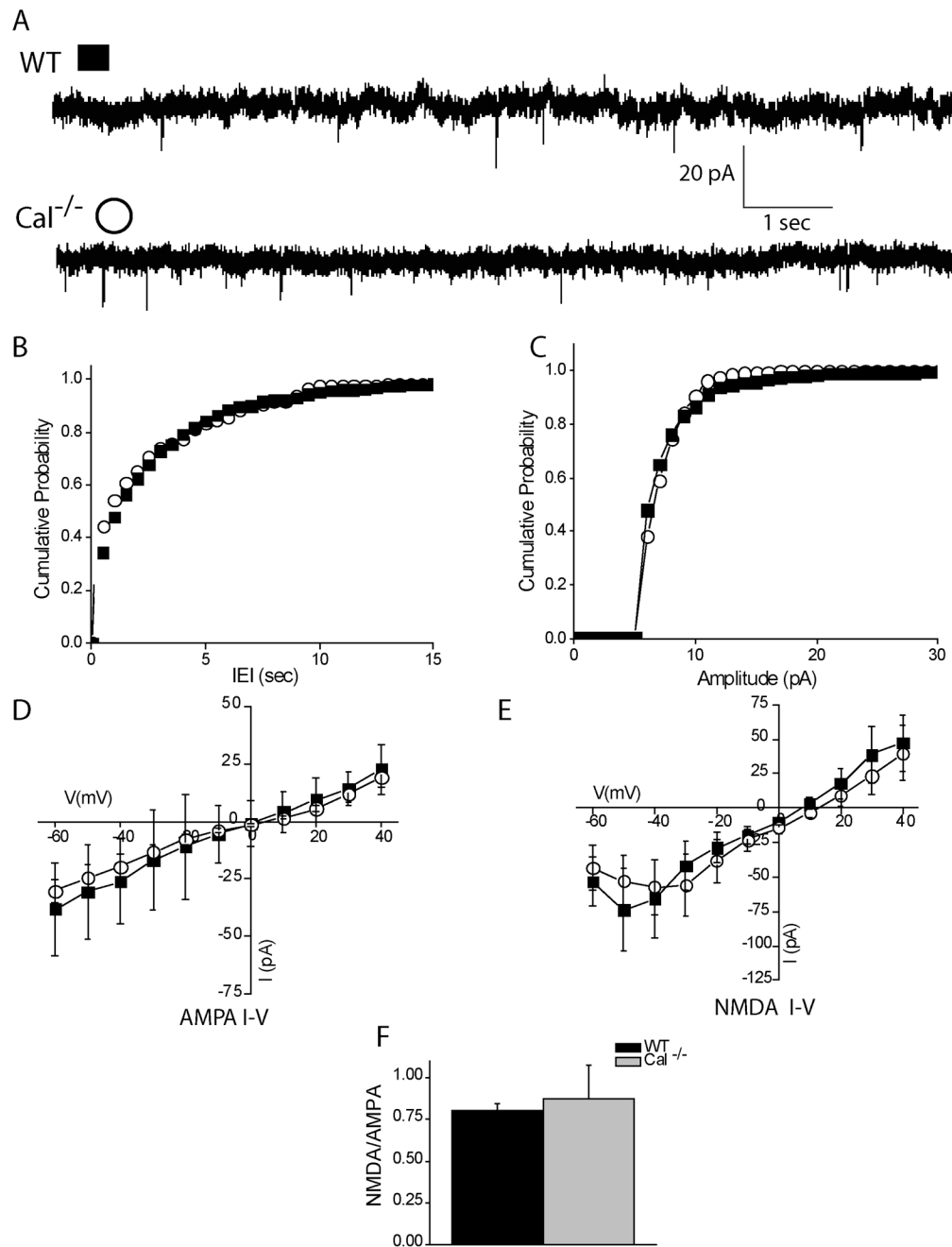


### Figure 3. Basal transmission is unaffected by calcyon deletion

(A) Sample traces of mEPSCs recorded in WT (left) and Cal<sup>-/-</sup> (right) CA1 neurons. Average mEPSC frequency (B) and amplitude (C) distribution detected in WT (n=8, age: P16-32) and Cal<sup>-/-</sup> (n=8, age: P16-P30) CA1 neurons. (D) I-V plots for evoked AMPA and (E) NMDA-mediated EPSCs recorded from CA1 neurons in WT (filled boxes, n=8, age: P16-P50) and Cal<sup>-/-</sup> (open circles, n=8, age: P14-P55) slices while holding cells at membrane potentials from -60 to +40 mV. I-V plots were obtained with D-APV (50 μM) (for AMPA current recording) or with CNQX (50 μM) (for NMDA currents) and bicuculline (10 μM) included in the bath. (F) Average NMDA/AMPA ratio of eEPSCs is similar in Cal<sup>-/-</sup> and WT animals.

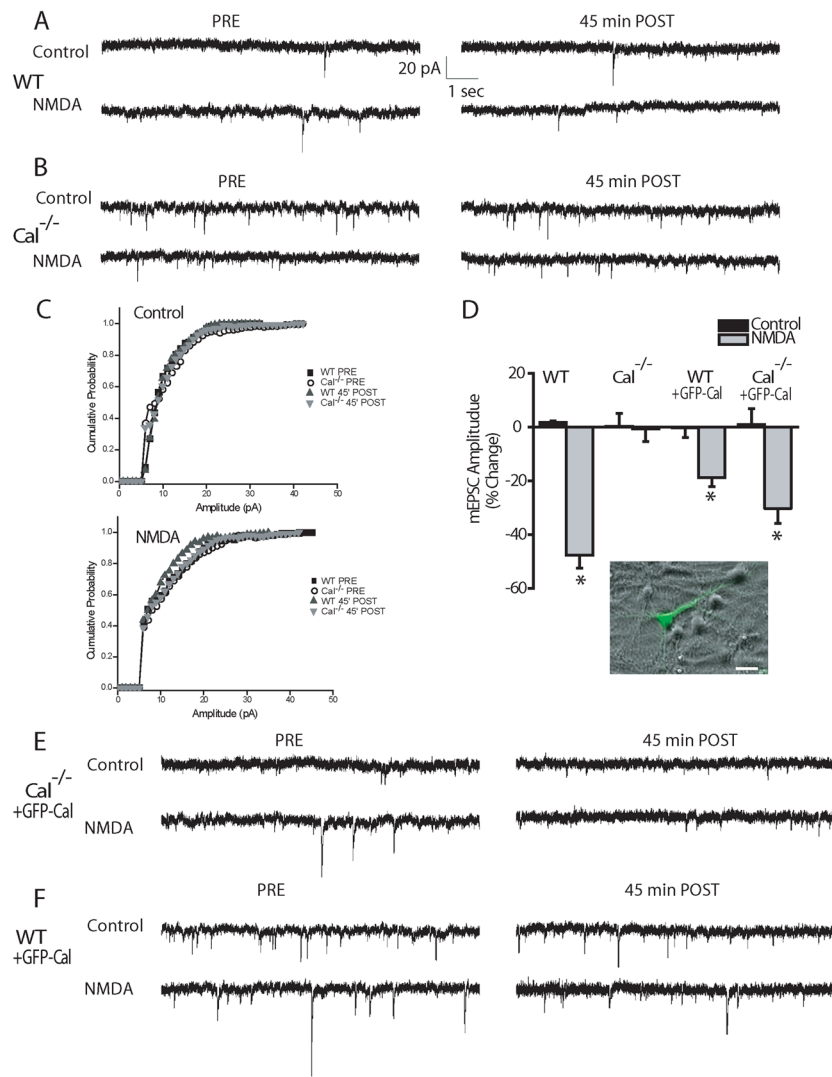


**Figure 4. Chemical LTD in primary hippocampal cultures is calcyon dependent** (Representative mEPSC traces from (A) WT and (B)  $Cal^{-/-}$  neurons before (left, black) and 45 min after (right, gray) NMDA application or control as indicated. Neurons in the WT cultures showed an immediate and prolonged significant decrease in mEPSC amplitude after chemical LTD induction. In contrast, no change in mEPSC amplitude was detected in  $Cal^{-/-}$  neurons following NMDA treatment. (C) Amplitude distributions for WT and  $Cal^{-/-}$  neurons before and after either control buffer (upper) or NMDA (lower) application. (D) Bar graph showing the mean and SEM of the percent change in mEPSC amplitude 35 to 45 min after 3 min application of NMDA (gray bars) or control treatment (black bars). Responses were normalized to pre-treatment values. (\*,  $p < .05$  following t-test of control and NMDA groups for each condition.) Inset below shows a GFP-Cal transfected neuron, bar = 30 micron. (E, F) Representative mEPSC traces from (E)  $Cal^{-/-}$  and (F) WT neurons. Transfection with GFP-Cal permitted LTD induction in  $Cal^{-/-}$  neurons. Scale is as in A, B.

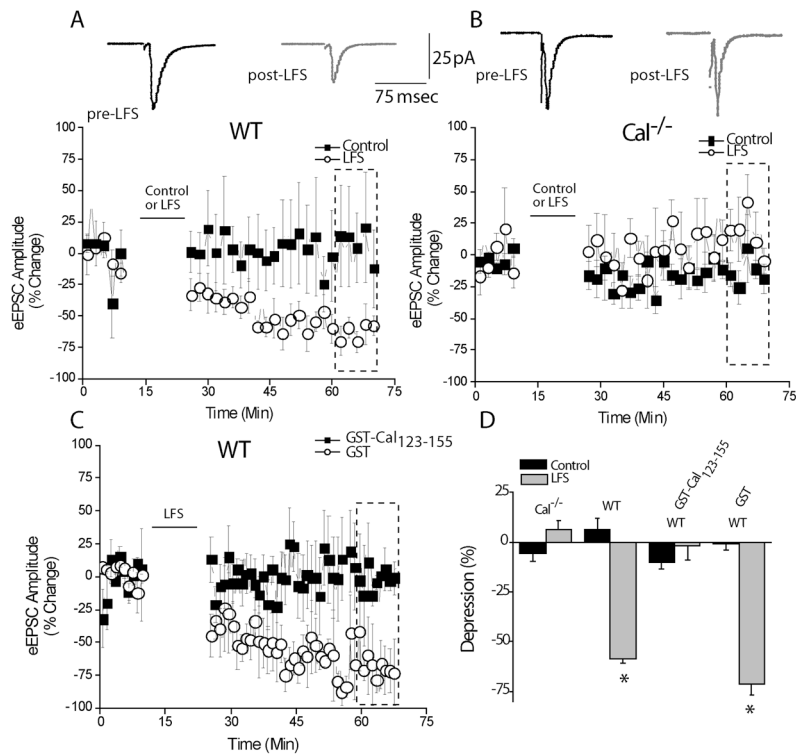


### Figure 5. LTD in acute hippocampal slices is calcyon dependent

Plot of eEPSC amplitude as a function of time for (A) Cal<sup>+/+</sup> (WT) and (B) Cal<sup>-/-</sup> CA1 neurons in response to control (0.03 Hz-control; filled squares) or LFS (1 Hz; open circles) stimulation delivered during the period indicated. Values are normalized to baseline amplitudes. WT neurons that received LFS (n=8, age: P16-P31) show an immediate and persistent decrease in eEPSC amplitude. In contrast, Cal<sup>-/-</sup> neurons receiving LFS (n=8, age: P17-P31) maintain stable eEPSC amplitudes for the length of the recording. After control stimulation, neither WT (n=8; age: P16-P32) nor Cal<sup>-/-</sup> (n=8; age: P16-P30) cells showed any significant change from baseline. Insets above time courses show representative traces (each composed of an average of 20 responses) in (A) WT and (B) Cal<sup>-/-</sup> cells before (black, left) and after (gray, right) LFS, respectively. (C) Time course of normalized eEPSC amplitudes recorded in WT cells with GST-Cal<sub>123-155</sub> (filled squares) or GST (open circles) included in the patch pipette during baseline and in response to LFS. (n=8 for all groups) (D) Bar graphs summarizing the time course data shown in 5A-C. The first two pairs of bars show the mean and SEM of the percent depression in eEPSC amplitude detected in WT and Cal<sup>-/-</sup> neurons during the 35 to 45 min period (indicated by a box in the time courses) following control (black bars) or LFS stimulation (gray bars). WT, but not Cal<sup>-/-</sup> cells that received LFS show a significant decrease in eEPSC amplitude (gray bar) compared to cells that were stimulated at 0.03 Hz (\*, p<.05; t-test). The two pairs of bars on the right show that adding GST-Cal<sub>123-155</sub> (0.6μM) to the recording pipette prevents LTD induction in WT cells. Conversely adding GST protein only (0.6μM) does not prevent LTD in WT cells.

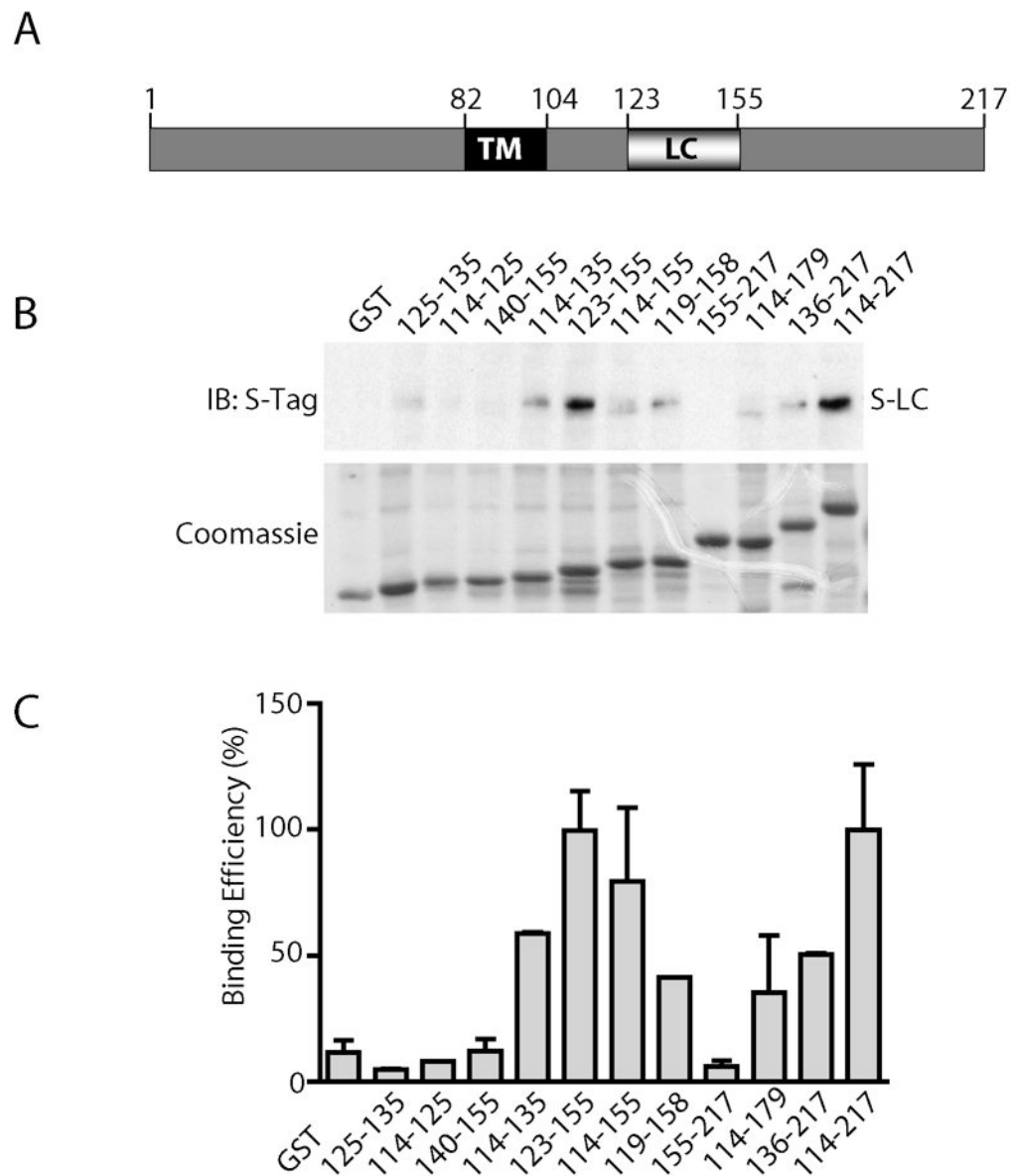


**Figure 6. Clathrin light chain binding domain in Calcyon**

(A) Stick diagram of calcyon, TM, transmembrane domain, LC, clathrin light chain binding region. Equimolar amounts of each GST-calcyon deletion construct was pre-bound to glutathione resin and tested for the ability to retain full length S-Tag-LC. (B) Immunoblot of pulled down material probed with S-Tag antibodies, and corresponding Coomassie stained gel showing input GST fusion proteins. (C) Histograms showing the S-LC binding efficiency of each GST-Cal fusion protein normalized to levels of S-LC bound by GST-Cal<sub>114-217</sub>. Bars show the mean binding efficiency, and error bars the SEM, obtained in 2 to 4 independent experiments for each construct.